

# Ligand effects on $\text{Si}_x\text{L}_y$ cluster structures with $\text{L} = \text{H}$ and $\text{F}$

YINGBIN GE and JOHN D. HEAD\*

Department of Chemistry, University of Hawaii, 2545 The Mall, Honolulu, HI 96822, USA

(Received 14 August 2004; accepted 18 October 2004)

The global minima for  $\text{Si}_2\text{L}_4$ ,  $\text{Si}_7\text{L}_{14}$ ,  $\text{Si}_8\text{L}_{14}$ ,  $\text{Si}_{10}\text{L}_{16}$  and  $\text{Si}_{10}\text{L}_{14}$  with  $\text{L} = \text{H}$  and  $\text{F}$  are determined at the B3LYP density functional theory level by using the cluster genetic algorithm (CGA) developed in our laboratory. We find the H and F ligands to produce very different low-energy  $\text{Si}_x\text{L}_y$  structures. In general,  $\text{Si}_x\text{H}_y$  prefers to form structures with H fairly evenly distributed over the Si atoms, whereas,  $\text{Si}_x\text{F}_y$  favours forming structures containing  $\text{SiF}_3$  side groups. These  $\text{SiF}_3$  side groups result in the  $\text{Si}_x\text{F}_y$  global minima having smaller Si rings with higher ring strain present than in the  $\text{Si}_x\text{H}_y$  global minima structures.

## 1. Introduction

Nanometer-sized silicon clusters have recently attracted considerable interest because they exhibit intense photoluminescence (PL) and have the potential of being developed into a practical optoelectronic device. The nanoparticles contrast with bulk silicon, which only shows a low-intensity PL owing to it being an indirect gap semiconductor. Quantum confinement [1, 2] and surface effect [3–6] theories have been proposed to explain the mechanism of the PL in silicon clusters. The progress in methods development, through the work of the Handy group and others, means that molecular quantum mechanics can now be used to calculate the optoelectronic properties for relatively large atomic and molecular clusters. For instance, Zhou, Friesner and Brus (ZFB) recently used density functional theory (DFT) to calculate the electronic structure for 1 to 2 nm diameter silicon clusters as large as  $\text{Si}_{87}\text{H}_{76}$  [6]. ZFB treated several different sized Si clusters passivated by either H, oxide, OH, hydrocarbon or F ligands. The calculations enable the characterization of single Si nanoparticles rather than the ensemble of particles with uncertain size ranges present in most real samples. In order to do these calculations, ZFB appear to make the chemically reasonable assumption that the most stable nanoclusters consist of a Si core with the same diamond-lattice-like structure as found in bulk Si. ZFB then passivate dangling surface Si bonds of the diamond-lattice-like core with a ligand of interest and perform a full local optimization to get the geometry of specific clusters. Degoli *et al.* make a similar diamond-lattice-like assumption in their ground and excited state

calculations on clusters ranging from  $\text{Si}_3\text{H}_{12}$  to  $\text{Si}_{35}\text{H}_{36}$  [7]. One of the reasons why quantum mechanical calculations are so useful in this research is because it is experimentally very difficult to determine the geometry of an individual cluster or even if a cluster has the anticipated stoichiometry. Unfortunately, a full local geometry optimization does not generally guarantee that the lowest possible energy structure and corresponding electronic properties for the cluster has been computed.

We have been developing strategies using a genetic algorithm (GA) for globally optimizing at the *ab initio* level  $\text{Si}_x\text{H}_y$  clusters [8–11]. The search procedure entails performing many local geometry optimizations of different cluster structures and we use a re-parametrized semi-empirical AM1 [12] method as a fast energy pre-screening method before using a relatively small number of *ab initio* calculations to identify the global minimum [9, 10]. Using a semi-empirical method, rather than some of the other available empirical potentials, avoids having to explicitly specify bond types present in the clusters. Thus each H atom in a  $\text{Si}_x\text{H}_y$  has the option of forming a bond with either a Si atom or another H atom depending on which bond gives a lower cluster energy. As a consequence, when a Si cluster is completely H-passivated, any remaining excess H atoms can pair up to form  $\text{H}_2$  molecules. By using this procedure we have demonstrated that the lowest energy structures for the clusters  $\text{Si}_{10}\text{H}_{16}$ ,  $\text{Si}_{14}\text{H}_{20}$  and  $\text{Si}_{18}\text{H}_{24}$  do consist of a diamond-lattice-like  $\text{Si}_x$  core fully passivated by H atoms as assumed by ZFB. However, our calculations also show that it should not be all that difficult to generate relatively stable under-H-passivated clusters  $\text{Si}_{10}\text{H}_{14}$ ,  $\text{Si}_{14}\text{H}_{18}$  and  $\text{Si}_{18}\text{H}_{22}$ , which, as figure 1 indicates, have very different  $\text{Si}_x$  core structures from the fully H-passivated clusters [10, 11]. The  $\text{Si}_x$  cores in the under-H-passivated clusters could be regarded as

\* Corresponding author. e-mail: johnh@hawaii.edu

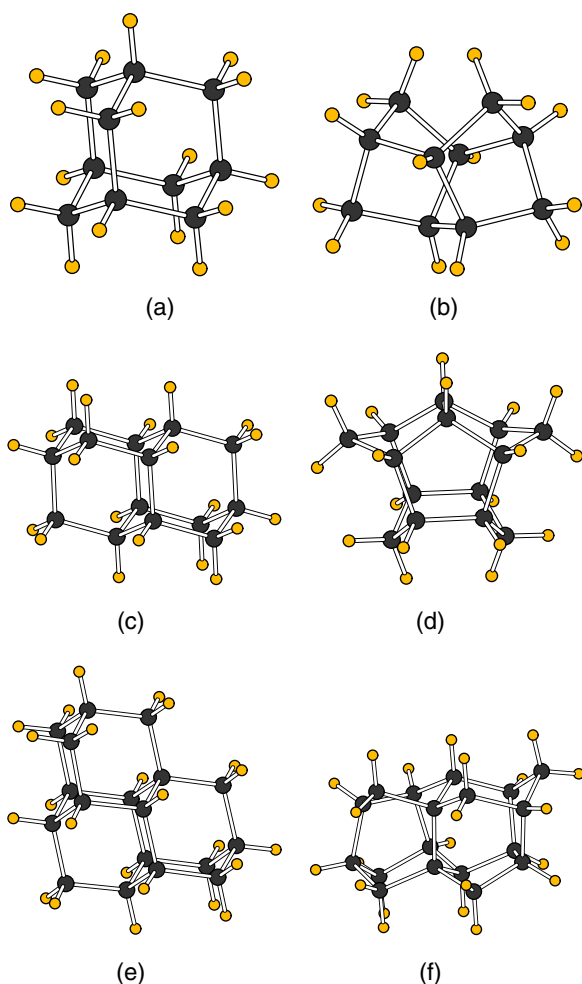


Figure 1. The MP2 global minima of various silicon hydride clusters: (a)  $\text{Si}_{10}\text{H}_{16}$ ; (b)  $\text{Si}_{10}\text{H}_{14}$ ; (c)  $\text{Si}_{14}\text{H}_{20}$ ; (d)  $\text{Si}_{14}\text{H}_{18}$ ; (e)  $\text{Si}_{18}\text{H}_{24}$ ; (f)  $\text{Si}_{18}\text{H}_{22}$ .

a defect in the bulk Si lattice and these defects could actually be the origin of the bright PL in Si nanoparticles. The under-H-passivated Si clusters demonstrate why global optimization methods are so important: their structures cannot be simply obtained by local optimization calculations initiated by simply removing two H atoms from the  $\text{Si}_{10}\text{H}_{16}$ ,  $\text{Si}_{14}\text{H}_{20}$  and  $\text{Si}_{18}\text{H}_{24}$  global minima.

We are in the process of extending our global optimization strategy to  $\text{Si}_x\text{L}_y$  clusters with other ligands L. One of the difficulties with going beyond H as the ligand L is that the semi-empirical energy evaluation becomes much slower. For instance, an AM1 calculation on  $\text{Si}_7\text{F}_{14}$  involves 84 valence basis functions, which is double the number of basis functions required by a  $\text{Si}_7\text{H}_{14}$  calculation. To speed up the semi-empirical calculations we have been investigating replacing the F ligand with a pseudo-H-like atom and using a

$\text{Si}_x\text{F}_y$  training set to get the F parameters. In this paper we report preliminary results using this strategy to find the low *ab initio* energy structures for the  $\text{Si}_7\text{F}_{14}$ ,  $\text{Si}_8\text{F}_{14}$ ,  $\text{Si}_{10}\text{F}_{14}$  and  $\text{Si}_{10}\text{F}_{16}$  clusters. Instead of needing to use a global optimization method, we had originally anticipated that we could find the lowest energy  $\text{Si}_x\text{F}_y$  structure by simply replacing the H atoms in the low-energy  $\text{Si}_x\text{H}_y$  clusters with F atoms. However, as our results below indicate, we find the ranking of the low-energy  $\text{Si}_x\text{F}_y$  structures to be very different to those found for  $\text{Si}_x\text{H}_y$ .

The rest of the paper is organized as follows. In the next section we outline the computational methods used. In the results and discussion section we compare the *ab initio* energies and structures for  $\text{Si}_2\text{L}_4$ ,  $\text{Si}_7\text{L}_{14}$ ,  $\text{Si}_8\text{L}_{14}$ ,  $\text{Si}_{10}\text{L}_{14}$  and  $\text{Si}_{10}\text{L}_{16}$  clusters with L = H and F. The final section of the paper contains concluding remarks.

## 2. Computation methods

The  $\text{Si}_x\text{L}_y$  cluster global optimizations are performed with our recently improved cluster genetic algorithm (CGA) [11]. The Deaven and Ho cut-and-paste mating method [13] along with three other mutation operators are applied to generate offspring from parents. The cut-and-paste method cuts two parent clusters into halves along randomly orientated planes and recombines two halves from different parents into an offspring structure. The first mutation operation removes a  $\text{SiL}_3$  group and replaces it with a single L atom and inserts a  $\text{SiL}_2$  group between two randomly selected neighbouring Si atoms to produce either a longer Si chain or an expanded Si ring. The second mutation operation is just the reverse procedure of the first one: it removes a  $\text{SiL}_2$  group from the cluster and then a randomly chosen L atom is replaced by a  $\text{SiL}_3$  group. To reduce making a drastic geometry change the two Si atoms which were neighbouring the  $\text{SiL}_2$  group are pulled slightly towards each other to induce the formation of a new Si–Si bond. The last operator, a piece-rotation mutation method, is a single-parent cut-and-paste operator and is similar to the operator used by Rata *et al.* [14] for the global optimization of Si-only clusters. The  $\text{Si}_x\text{L}_y$  cluster is randomly cut into two parts and then one half of the cluster is randomly rotated relative to the other half. The above four genetic operators are applied with equal probability.

The global optimization starts from 120 randomly generated locally optimized structures as the ancestor population. The fitness value of an individual cluster is taken as the GAM1 semi-empirical energy of the locally optimized cluster. Tournament selection is used to select

the parents needed to produce offspring. Since the calculations are performed on either a 16 or a 32 processor computer we do not explicitly treat separate generations. The CGA performs parent selection, mating/mutation process and generates a new trial offspring structure as soon as the local geometry optimization of a cluster included in the parent population is finished on a processor. To avoid identical structures dominating the population, new offspring which already exist in the current population are discarded. The final set of clusters with lowest GAM1 energies are locally optimized with *ab initio* calculations.

All of the pre-screening semi-empirical calculations were performed using the GAMESS program [15]. Since we only examine well passivated  $\text{Si}_x\text{L}_y$  clusters we use the GAM1 semi-empirical parameters obtained previously from the  $\text{Si}_7\text{H}_{14}$  training set [10] for the  $\text{Si}_x\text{H}_y$  clusters. We have also derived Si and F GAM1 semi-empirical parameters for the  $\text{Si}_x\text{F}_y$  clusters using a pseudo-H-like atom and a  $\text{Si}_7\text{F}_{14}$  training set which will be described in more detail elsewhere [16]. Since we are

searching for accurate low-energy clusters of fairly large  $\text{Si}_x\text{L}_y$  clusters, *ab initio* calculations were performed with the DFT method using the B3LYP functional [17] and the Gaussian package [18]. We used the LanL2dz(d) scheme consisting of the Hay–Wadt effective core potential (ECP) and valence basis set for Si [19] augmented with a *d* function ( $\zeta_d = 0.45$ ) [20] and the Dunning–Hay basis for H and F. Because of the strong F electronegativity the F basis set was augmented with a *p* diffuse function ( $\zeta_p = 0.074$ ) and a *d* polarization function ( $\zeta_d = 0.90$ ) [21]. The accuracy of the B3LYP energy ranking for some of the smaller clusters was checked against MP2 [22] calculations performed using the GAMESS program.

### 3. Results and discussion

#### 3.1. $\text{Si}_2\text{L}_4$

Only two  $\text{Si}_2\text{L}_4$  local minimum types are possible when the ligand L binds to just one of the Si atoms, as shown in figure 2. The disilene  $\text{L}_2\text{Si}=\text{SiL}_2$  isomer is not a

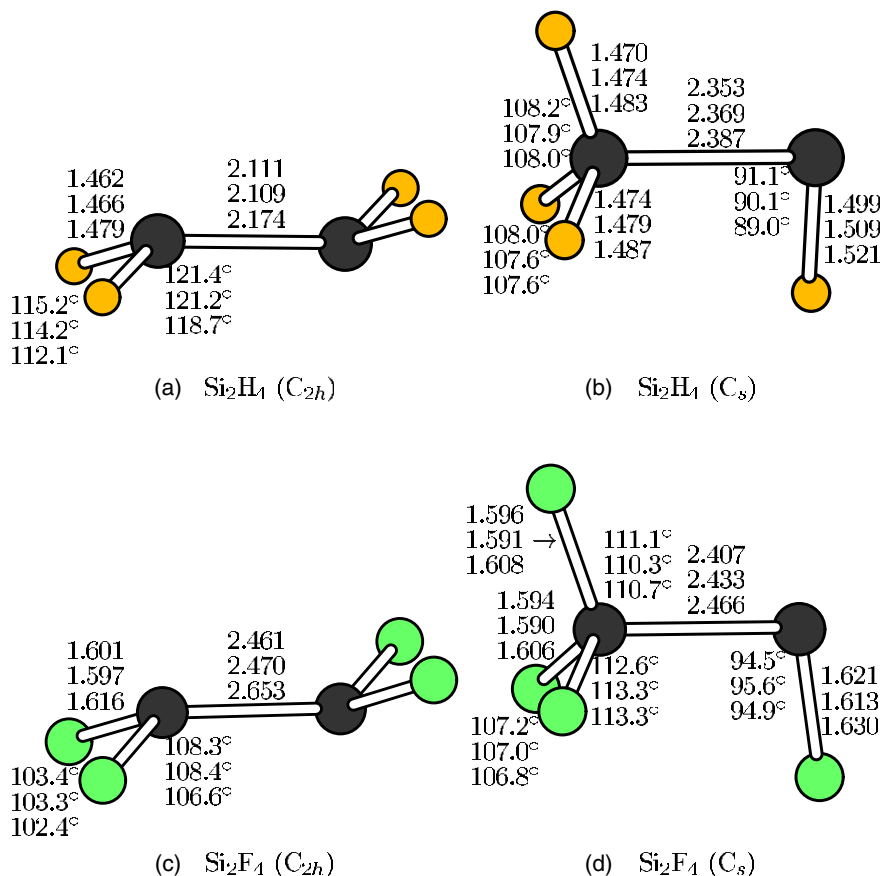


Figure 2. The locally optimized  $\text{Si}_2\text{H}_4$  and  $\text{Si}_2\text{F}_4$  isomers. The  $\text{Si}_2\text{H}_4$  geometry information is listed from top to bottom in the order: MP2/LanL2dz(d), B3LYP/LanL2dz(d) and CCSD(T)/cc-pVTZ [23] methods. The  $\text{Si}_2\text{F}_4$  geometry information is in the order: MP2/LanL2dz(d), B3LYP/LanL2dz(d) and B3LYP/DZP++(d) [24] methods.

Table 1. Relative energies for the two  $\text{Si}_2\text{F}_4$  and  $\text{Si}_2\text{H}_4$  isomers with  $C_{2h}$  and  $C_s$  symmetry shown in figure 2. Listed are the MP2 and B3LYP optimized energies for various basis sets and the CCSD(T) single point energy computed with the B3LYP optimized geometry. All energies are in  $\text{kcal mol}^{-1}$ .

Isomer	LanL2dz(d)			6-311 + G(d)			6-311 + G(3df)		
	MP2	B3LYP	CCSD(T)	MP2	B3LYP	CCSD(T)	MP2	B3LYP	CCSD(T)
$\text{F}_2\text{SiSiF}_2$	0.0	0.0	0.0	0.0	0.0	0.0	0.0	0.0	0.0
$\text{FSiSiF}_3$	-12.7	-8.1	-10.2	-11.0	-6.4	-9.3	-11.5	-6.7	NA
$\text{H}_2\text{SiSiH}_2$	0.0	0.0	0.0	0.0	0.0	0.0	0.0	0.0	0.0
$\text{HSiSiH}_3$	12.1	10.5	11.9	8.5	5.8	8.8	9.6	6.2	8.5

simple analogue of ethylene and instead favours forming a *trans*-bent structure with  $C_{2h}$  symmetry. However, even with this relatively small molecule, the preferred lowest energy isomer varies with the different H or F ligand. Recent work by Sari *et al.* provides an extensive review of past work on the different  $\text{Si}_2\text{H}_4$  isomers and they use highly correlated *ab initio* coupled cluster theories [23] to predict that the silene  $\text{H}_2\text{Si}=\text{SiH}_2$  is  $6 \text{ kcal mol}^{-1}$  more stable than  $\text{HSi}-\text{SiH}_3$ . Table 1 shows that our calculations on  $\text{Si}_2\text{H}_4$  using LanL2dz(d) MP2, B3LYP and CCSD(T) give results which are reasonably consistent with the Sari *et al.* results. Fewer calculations appear to have previously been performed on the  $\text{Si}_2\text{F}_4$  species. Li *et al.* used DFT methods with various functionals to investigate structures, thermochemistry and electron affinities for the  $\text{Si}_2\text{F}_n$  ( $n = 1 - 6$ ) series [24]. Consistent with the Li *et al.* work, our calculations, which are summarized in table 1, find the fluorinated disilene ( $C_{2h}$ ) is now less stable than  $\text{FSi}-\text{SiF}_3$  ( $C_s$ ) by  $6-12 \text{ kcal mol}^{-1}$  depending on the method used.  $\text{Si}_2\text{F}_4$  represents the upper limit to the system size we can treat using highly correlated *ab initio* methods with our available computing resources and table 1 demonstrates that the LanL2dz(d)/B3LYP calculations should give adequate results for the larger clusters described in the rest of the paper. The important observation from these  $\text{Si}_2\text{L}_4$  calculations is that the F ligand appears to favour forming a trifluorosilyl,  $\text{SiF}_3$ , group, whereas the H ligand prefers to be evenly distributed on the two Si atoms. This F preference for forming  $\text{SiF}_3$  groups while H favours being more evenly dispersed on all of the available Si atoms turns out to be a common theme in the global minima structures described below for the larger  $\text{Si}_x\text{L}_y$  clusters.

### 3.2. $\text{Si}_7\text{L}_{14}$

Our original motive for examining the relative energies of different  $\text{Si}_7\text{H}_{14}$  clusters was to develop a training set which could be used in a parametrization genetic algorithm to obtain improved AM1 parameters, which

we designated as GAM1 parameters, for the Si atoms in fully passivated  $\text{Si}_x\text{H}_y$  clusters [10].  $\text{Si}_7\text{H}_{14}$  is large enough that it can adopt various configurations, ranging from linear through three- to seven-membered Si ring structures, which represent common partial structures found in a well-passivated  $\text{Si}_x\text{H}_y$  cluster. In figure 3 we show the locally optimized structures and relative energies for the  $\text{Si}_7\text{F}_{14}$  cluster obtained after replacing all the H atoms with F in our previous set of 14  $\text{Si}_7\text{H}_{14}$  training compounds. To illustrate the change in relative energies of the silicon fluorides we still order the  $\text{Si}_7\text{F}_{14}$  structures in figure 3 in the original energy ranking order we obtained for  $\text{Si}_7\text{H}_{14}$  with MP2/6-31G\* calculations. Structures 3(a) through 3(g) contain either five- or six-membered Si rings which, for  $\text{Si}_7\text{H}_{14}$ , have an energy spread of  $2 \text{ kcal mol}^{-1}$ . Previously, we found with MP2/6-31G\* calculations the five-membered Si ring structure 3(a) to be the global minimum and  $0.8$  and  $1.3 \text{ kcal mol}^{-1}$  more stable than structures 3(b) and 3(c) [10]. There is clearly still a small energy difference between the five- and six-membered Si ring  $\text{Si}_7\text{H}_{14}$  structures, but it is reversed, when B3LYP/LanL2dz(d) and MP2/LanL2dz(d) calculations are performed. Consistent with an increase in strain with reduced ring size, the  $\text{Si}_7\text{H}_{14}$  relative *ab initio* energies for the 3(l) and 3(m) structures with four- and three-membered Si rings present are around  $10$  and  $23 \text{ kcal mol}^{-1}$ , respectively, higher in energy. In strong contrast for  $\text{Si}_7\text{F}_{14}$  the five-membered Si ring structure 3(a) is approximately  $20 \text{ kcal mol}^{-1}$  lower in energy than the two structures 3(b) and 3(c) containing a six-membered Si ring. Figure 3 also shows significant changes in the energy rankings for many of the other  $\text{Si}_7\text{F}_{14}$  isomers. Due to the much larger Si-F bond energy relative to the F-F and Si-Si bond energies, structure 3(k) shows that the Si clusters should favour high passivation by F atoms.

We have used the  $\text{Si}_7\text{F}_{14}$  B3LYP energies to obtain GAM1 parameters for Si and F. These parameters were then used in the CGA to search for the  $\text{Si}_7\text{F}_{14}$  global minimum and other low-energy structures which

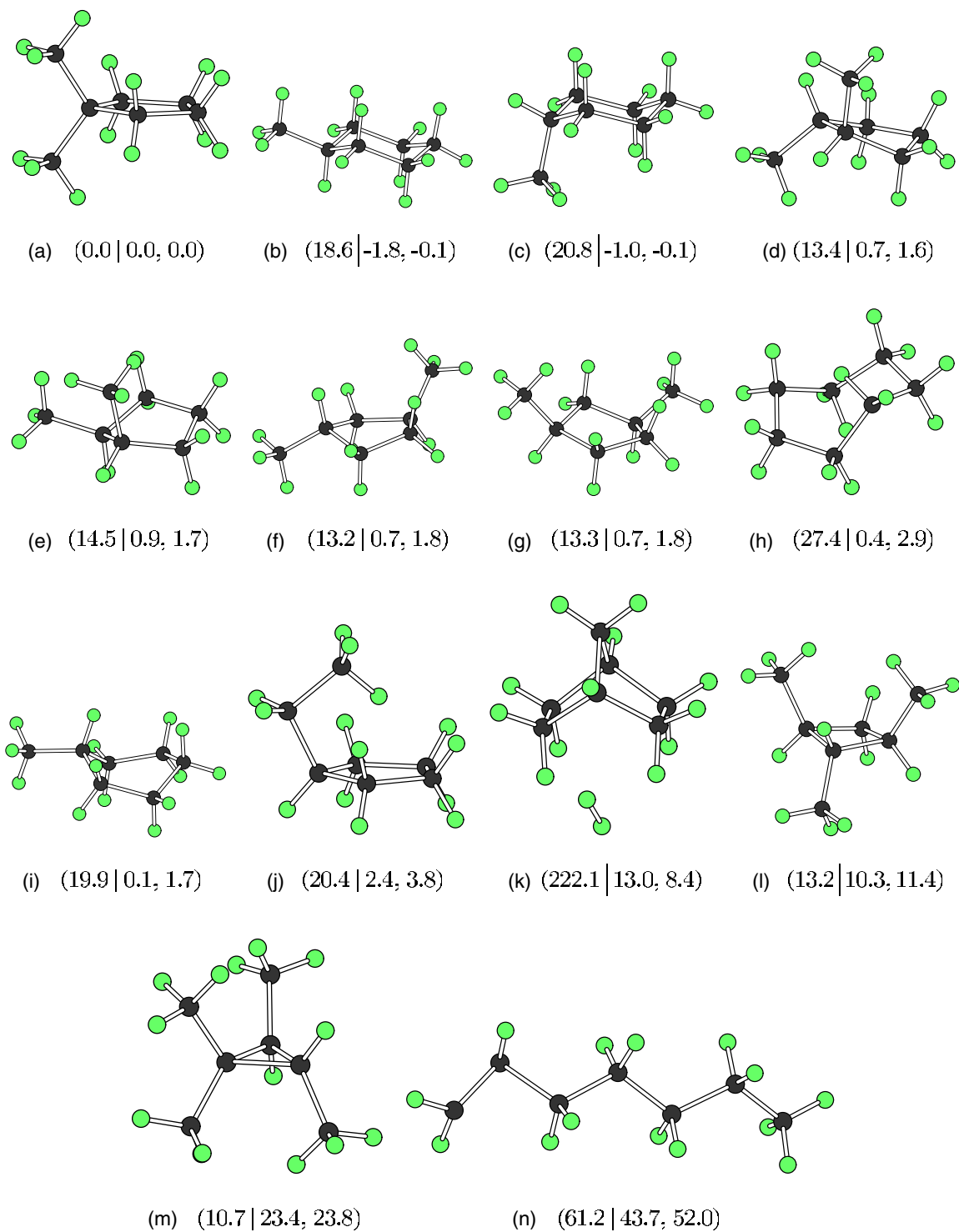


Figure 3. The  $\text{Si}_7\text{F}_{14}$  B3LYP locally optimized geometries for the original 14 training set compounds. In parentheses: ( $\text{Si}_7\text{F}_{14}$  B3LYP relative energy | corresponding  $\text{Si}_7\text{H}_{14}$  B3LYP and MP2 relative energies). All energies are in  $\text{kcal mol}^{-1}$ .

ultimately should be included in the  $\text{Si}_7\text{F}_{14}$  training set. In figure 4 we show three new  $\text{Si}_7\text{F}_{14}$  structures found by the CGA with even lower B3LYP energies than those obtained for the original training set clusters. Structure

4(a) is the  $\text{Si}_7\text{F}_{14}$  B3LYP/LanL2dz(d) global minimum and in figure 4 we now take structure 4(a) energy as the zero reference. Structures 4(a) and 4(b) consist of a four-membered Si ring with three trifluorosilyl

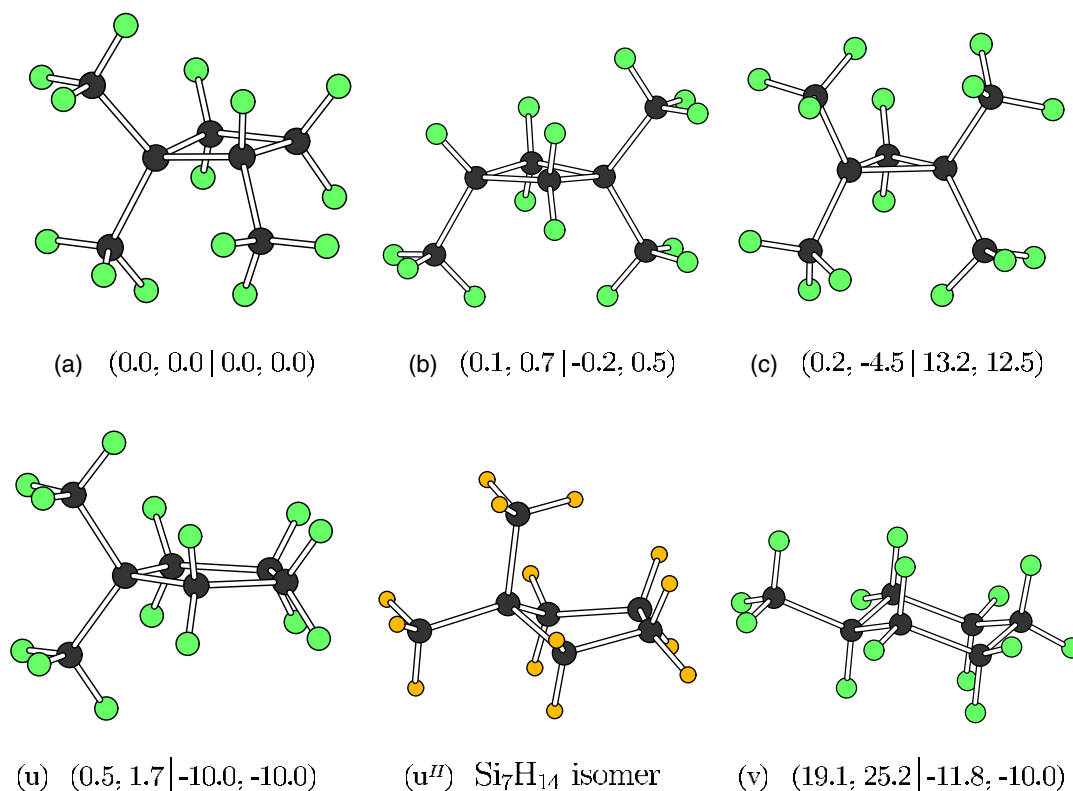


Figure 4. The B3LYP locally optimized geometries of the three low-energy Si<sub>7</sub>F<sub>14</sub> clusters obtained by the CGA using the Si and F GAM1 parameters. (u) and (v) are Si<sub>7</sub>F<sub>14</sub> clusters containing five- and six-membered Si rings, respectively; (u<sup>H</sup>) is the Si<sub>7</sub>H<sub>14</sub> global minimum. In parentheses: (Si<sub>7</sub>F<sub>14</sub> B3LYP and MP2 relative energies | Si<sub>7</sub>H<sub>14</sub> B3LYP and MP2 relative energies). All energies are in kcal mol<sup>-1</sup>.

groups attached, while 4(c), at only slightly higher B3LYP energy but a lower MP2 energy, contains a three-membered Si ring with four SiF<sub>3</sub> groups attached. We include in figure 4 the five-membered Si ring global minimum 4(u<sup>H</sup>) and the lowest energy six-membered ring 4(v) structures for Si<sub>7</sub>H<sub>14</sub>. Remarkably, in the local geometry optimizations we have found F to only slightly perturb the Si<sub>7</sub> frameworks from their original Si<sub>7</sub>H<sub>14</sub> positions. The only major exception to this is found for the low-energy non-planar five-membered ring Si<sub>7</sub>H<sub>14</sub>, structure 4(u<sup>H</sup>) in figure 4, which becomes planar in Si<sub>7</sub>F<sub>14</sub>. The energies of the Si<sub>7</sub>H<sub>14</sub> structures 3(l) and 3(m) suggest there must be a large ring strain present in the four- and three-membered Si<sub>7</sub>F<sub>14</sub> rings, but this must now be compensated by forming the three or four trifluorosilyl groups. In general, figure 3 and 4 show that the Si<sub>7</sub>F<sub>14</sub> structures with the greater number of SiF<sub>3</sub> groups have the lower energies. For the series of Si<sub>7</sub>F<sub>14</sub> structures containing five-membered rings we find the relative energy ordering: two SiF<sub>3</sub> groups attached to same Si ring atom 3(a) < two SiF<sub>3</sub> groups attached to different Si ring atoms 3(d)–(g) < Si<sub>2</sub>F<sub>5</sub> group attached to single Si ring atom 3(j). This type of analysis can be

used to rationalize the relative energies of the other structures.

### 3.3. Si<sub>8</sub>L<sub>14</sub>

As an initial test of the transferability of the GAM1 Si and F parameters from the Si<sub>7</sub>F<sub>14</sub> training set to larger clusters with the same degree of F passivation we applied the CGA to find the global minimum for Si<sub>8</sub>F<sub>14</sub>. We also determined the Si<sub>8</sub>H<sub>14</sub> global minimum using separate CGA runs and the GAM1 Si parameters from the Si<sub>7</sub>H<sub>14</sub> training set. In figure 5 we show the eight Si<sub>8</sub>F<sub>14</sub> structures with the lowest B3LYP energies which are within 10 kcal mol<sup>-1</sup> of the global minimum structure 5(a) which we take as the zero energy reference. Included in figure 5 are two higher energy Si<sub>8</sub>F<sub>14</sub> structures 5(u) and 5(v) which we find as the Si<sub>8</sub>H<sub>14</sub> B3LYP and MP2 global minimum and the next lowest energy structures, respectively. Structure 5(b) is the second lowest Si<sub>8</sub>F<sub>14</sub> and the third lowest Si<sub>8</sub>H<sub>14</sub> B3LYP energy structure. Again we observe that the Si<sub>8</sub>H<sub>14</sub> and Si<sub>8</sub>F<sub>14</sub> global minimum structures are very different to each other. However, the H and F ligands

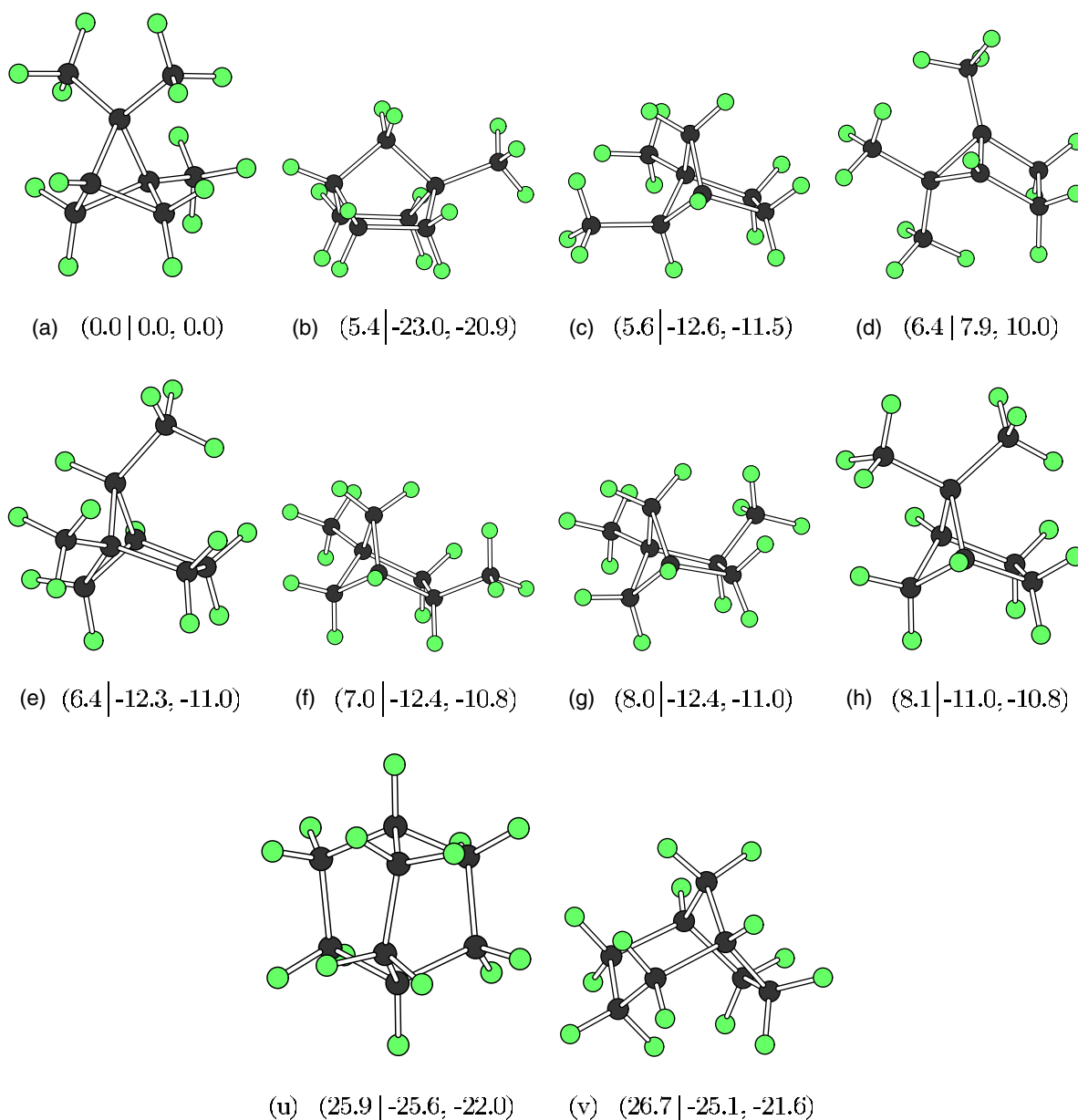


Figure 5. The B3LYP locally optimized geometries for the  $\text{Si}_8\text{F}_{14}$  low-energy clusters located by the CGA. Structures (u) and (v) correspond to the lowest energy  $\text{Si}_8\text{H}_{14}$  clusters. In parentheses: ( $\text{Si}_8\text{F}_{14}$  B3LYP relative energy |  $\text{Si}_8\text{H}_{14}$  B3LYP and MP2 relative energies). All energies are in  $\text{kcal mol}^{-1}$ .

cause structural changes similar to those we have already found in  $\text{Si}_2\text{L}_4$  and  $\text{Si}_7\text{L}_{14}$ . The H atoms in the low-energy  $\text{Si}_8\text{H}_{14}$  are evenly spread over all the Si atoms and five- and six-membered Si rings with low strain are formed. Structure 5(b) can be derived from 5(v) by moving a  $\text{SiL}_2$  group from the six-membered Si ring to produce the  $\text{SiL}_3$  group and the five-membered ring in 5(b). The low-energy  $\text{Si}_8\text{F}_{14}$  structures have up to three  $\text{SiF}_3$  side groups and, as a consequence, smaller three- or four-membered Si rings are present in these structures. The  $\text{Si}_8\text{F}_{14}$  global minimum 5(a) shows again

that trifluorosilyl groups attached to the same Si atom is energetically favoured despite the strain caused by the presence of four-membered Si rings. In contrast, structure 5(b) is formed from five- and six-membered Si rings which should have only a small amount of ring strain and, as a consequence, the single  $\text{SiF}_3$  group is able to lower its energy relative to the other structures containing more  $\text{SiF}_3$  groups. A similar analysis can be performed for structures 5(d,e). Structure 5(d) contains the strained three- and four-membered Si rings, but this is compensated by having two  $\text{SiF}_3$  attached to one Si

atom and another  $\text{SiF}_3$  group bonded to a different Si atom, whereas structure 5(e) should have less ring strain, but its relative energy is only stabilized by the presence of two  $\text{SiF}_3$  groups.

### 3.4. $\text{Si}_{10}\text{L}_{16}$

This is the smallest cluster where the  $\text{Si}_{10}$  core can adopt the bulk Si diamond-lattice-like structure. Each Si atom in the  $\text{Si}_{10}\text{L}_{16}$  diamond-lattice-like structure is tetrahedrally coordinated by other Si or L atoms and the six-membered Si rings should have little, if any, Si ring strain. As assumed by ZFB and Degoli *et al.* and others, it is very chemically reasonable to assume that the global minimum for the  $\text{Si}_{10}\text{L}_{16}$  is a diamond-lattice-like structure. We have now performed an extensive series of global optimization studies on the  $\text{Si}_{10}\text{H}_{16}$  stoichiometry, and computed GAM1, MP2 and B3LYP locally optimized geometries for a wide variety of different  $\text{Si}_{10}\text{H}_{16}$  structures and conclude that the diamond-lattice-like structure 6(u), in figure 6, is the *ab initio* global minimum [8, 10, 11]. The fact that our current CGA strategy [10, 11] is able to find diamond-lattice-like structures for  $\text{Si}_{14}\text{H}_{20}$  and  $\text{Si}_{18}\text{H}_{24}$  as well as  $\text{Si}_{10}\text{H}_{16}$  enhances our confidence with the CGA method at being able to find the correct global minimum for other stoichiometries which do not have a diamond-lattice-like structure as the global minimum. In figure 6 we show the B3LYP global minimum, structure 6(a), for  $\text{Si}_{10}\text{F}_{16}$  using the CGA and the Si and F GAM1 parameters for energy pre-screening. Also included in figure 6 are the different locally optimized B3LYP  $\text{Si}_{10}\text{F}_{16}$  structures within  $10\text{ kcal mol}^{-1}$  of the global minimum found by the CGA procedure. Once again  $\text{Si}_{10}\text{H}_{16}$  and  $\text{Si}_{10}\text{F}_{16}$  have vastly different low-energy structures. The H atoms in  $\text{Si}_{10}\text{H}_{16}$  prefer to be spread evenly over the  $\text{Si}_{10}$  core, while the F atoms favour forming trifluorosilyl groups in the low-energy  $\text{Si}_{10}\text{F}_{16}$  structures. As a consequence the fluorinated  $\text{Si}_{10}$  core contains some four-membered Si rings which are stabilized by the one or two  $\text{SiF}_3$  groups attached to the ring Si atoms. For both the H and F ligands there are two series of structures, 6(a–c) and 6(e–i,k), which have a narrow energy range, presumably because the members of each series contain a similar  $\text{Si}_8$  core and two  $\text{SiL}_3$  groups attached at different Si core positions. It is interesting that in all of the low-energy  $\text{Si}_{10}\text{F}_{16}$  structures shown in figure 6 each of the  $\text{SiF}_3$  groups bond with a core Si atom which is in turn bonded to three other Si core atoms. Structures 6(a–l) were all taken from the  $\text{Si}_{10}\text{F}_{16}$  CGA and the  $\text{Si}_{10}\text{H}_{16}$  optimized energies were obtained by replacing all F atoms by H atoms. When we examine the positions of the  $\text{SiH}_3$  groups found in low-energy structures obtained by the

$\text{Si}_{10}\text{H}_{16}$  CGA runs we do find examples of the silyl group bonding to Si core atoms which are also bonded to other H atoms and not just three other Si core atoms [10]. Obviously, a Si core atom already bonded to a strongly electronegative F atom is going to have less electrons available than a Si core atom only bonding to other Si core atoms. When one takes into consideration the low-energy structures found for  $\text{Si}_2\text{F}_4$ ,  $\text{Si}_7\text{F}_{14}$  and  $\text{Si}_8\text{F}_{14}$  and the energy stability gained by forming a  $\text{SiF}_3$  group, the 6(a) global minimum structure for  $\text{Si}_{10}\text{F}_{16}$  does become chemically reasonable even though it is very different from the diamond-lattice-like  $\text{Si}_{10}\text{H}_{16}$  global minimum.

### 3.5. $\text{Si}_{10}\text{L}_{14}$

One important decision when performing calculations on this passivated Si cluster is deciding how many ligands are needed to adequately passivate the Si core. In the introduction we noted that one of the reasons for using the AM1-based semi-empirical method is that it automatically enables  $\text{L}_2$  to be lost from the cluster if there is an excess of the passivating ligands. In our previous work we have examined the energetics of  $\text{Si}_{10}\text{H}_{16}$  losing  $\text{H}_2$  and have concluded this may be only favoured at high temperatures [8, 10]. To determine the energy of the  $\text{H}_2$  loss reaction we have determined the  $\text{Si}_{10}\text{H}_{14}$  global minimum. In figure 7 we show the low B3LYP energy structures obtained in the global optimization of  $\text{Si}_{10}\text{H}_{14}$  and  $\text{Si}_{10}\text{F}_{14}$  using the CGA. We have previously noted that the  $\text{Si}_{10}\text{H}_{14}$  global minimum 7(u) cannot be obtained by simply removing two H atoms from the  $\text{Si}_{10}\text{H}_{16}$  global minimum and then performing a local geometry optimization. To maintain an even distribution of H atoms the low-energy  $\text{Si}_{10}\text{H}_{14}$  cluster compensates for the reduced H passivation by forming structures containing some five- and even a four-membered Si rings. We find structure 7(a) as the  $\text{Si}_{10}\text{F}_{14}$  global minimum. It appears to adjust to the lower F passivation by only slightly reducing the Si ring sizes relative to  $\text{Si}_{10}\text{F}_{16}$  and instead 7(a) now contains a single trifluorosilyl group. In figure 7 we show the  $\text{Si}_{10}\text{F}_{14}$  structures which are within  $10\text{ kcal mol}^{-1}$  of the global minimum and do not find any structures containing two trifluorosilyl groups, presumably because these structures would have appreciably higher Si ring strain. Analogous to what we found for  $\text{Si}_{10}\text{L}_{16}$ , we find three series of structures, 7(a–c), 7(d,e,h), and 7(f,g,j), with narrow energy ranges, where each series consist of the same basic  $\text{Si}_9$  core framework, but with the  $\text{SiL}_3$  group bound at different Si core atom positions. We find the Si core atoms which bond with  $\text{SiF}_3$  to be coordinated by three other Si atoms. Overall, because of the much weaker F–F and Si–Si bond

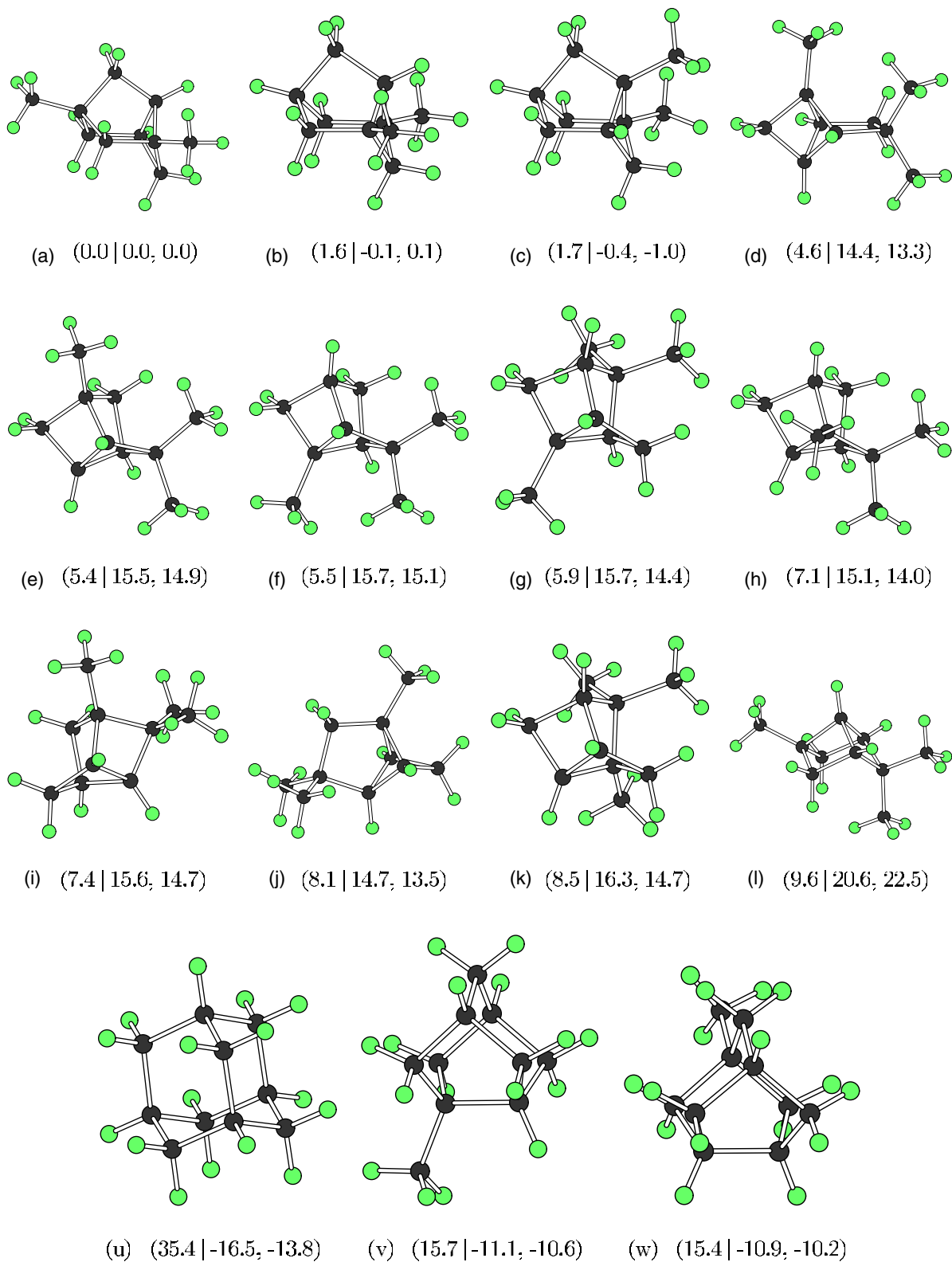


Figure 6. The  $Si_{10}F_{16}$  low-energy B3LYP locally optimized geometries located by the CGA on  $Si_{10}F_{16}$ . Structure (u) is the global minimum and (v) and (w) are low-energy structures for  $Si_{10}H_{16}$ . In parentheses: ( $Si_{10}F_{16}$  B3LYP relative energy |  $Si_{10}H_{16}$  B3LYP and MP2 relative energies). All energies are in  $\text{kcal mol}^{-1}$ .

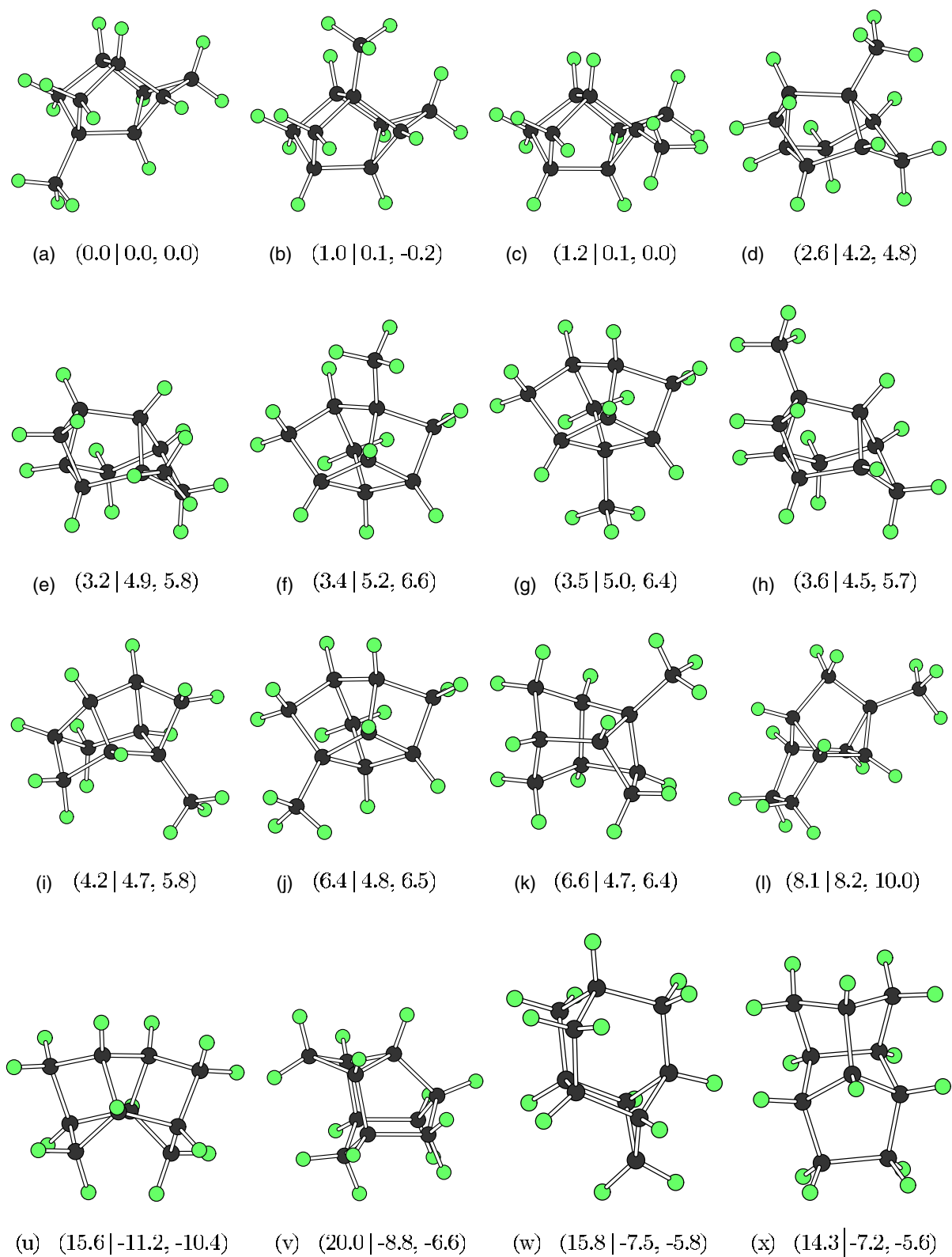


Figure 7. The  $\text{Si}_{10}\text{F}_{14}$  low-energy B3LYP locally optimized geometries located by the CGA. Structures (u)–(x) are the  $\text{Si}_{10}\text{H}_{14}$  global minimum and low-energy structures. In parentheses: ( $\text{Si}_{10}\text{F}_{14}$  B3LYP relative energy |  $\text{Si}_{10}\text{H}_{14}$  B3LYP and MP2 relative energies). All energies are in  $\text{kcal mol}^{-1}$ .

energies relative to the Si–F bond we do not anticipate that  $\text{Si}_{10}\text{F}_{16}$  will readily lose  $\text{F}_2$ .

#### 4. Conclusion

This study demonstrates that the global minima structures for  $\text{Si}_x\text{H}_y$  and  $\text{Si}_x\text{F}_y$  clusters are very different to each other. We have determined the global minima for  $\text{Si}_2\text{L}_4$ ,  $\text{Si}_7\text{L}_{14}$ ,  $\text{Si}_8\text{L}_{14}$ ,  $\text{Si}_{10}\text{L}_{16}$  and  $\text{Si}_{10}\text{L}_{14}$  with  $\text{L} = \text{H}$  and  $\text{F}$  by using the cluster genetic algorithm (CGA) developed in our laboratory. Our results show that the low-energy  $\text{Si}_x\text{F}_y$  clusters cannot be guaranteed to be identified by simply replacing the H atoms in low-energy  $\text{Si}_x\text{H}_y$  clusters by F and then performing a local geometry optimization.

In the low-energy well-H-passivated Si clusters, the H atoms prefer to be fairly evenly distributed over all the Si core atoms enabling five- and six-membered Si rings with little ring strain to be formed. As a consequence, clusters with the appropriate stoichiometry, such as  $\text{Si}_{10}\text{H}_{16}$ , have global minima with the Si cores resembling the diamond-lattice structure in bulk Si, as might be anticipated by chemical intuition. In contrast, the low-energy well-F-passivated Si clusters like to form structures containing one or more trifluorosilyl groups at the energy expense of forming highly strained four- and even three-membered Si rings. The trend of the different  $\text{Si}_x\text{F}_y$  clusters favouring the formation of  $\text{SiF}_3$  groups means that the  $\text{Si}_{10}\text{F}_{16}$  global minimum with strained five- and four-membered Si rings in the Si core found by the CGA is also chemically reasonable.

#### Acknowledgement

We are grateful for the generous supply of computer time provided by the Maui High Performance Computing Center.

#### References

[1] L.T. Canham, *Appl. Phys. Lett.*, **57**, 1046 (1990).

- [2] W.L. Wilson, P.F. Szajowski, L.E. Brus, *Science*, **262**, 1242 (1993).
- [3] M.V. Wolkin, J. Jorne, P.M. Fauchet, G. Allan, C. Delerue, *Phys. Rev. Lett.*, **82**, 197 (1999).
- [4] F. Zhou, J.D. Head, *J. Phys. Chem. B*, **104**, 9981 (2000).
- [5] A.B. Filonov, S. Ossicini, F. Bassani, F.A. d'Avitaya, *Phys. Rev. B*, **65**, 195317 (2002).
- [6] Z. Zhou, R.A. Friesner, L. Brus, *J. Am. Chem. Soc.*, **125**, 15599 (2003).
- [7] E. Degoli, G. Cantele, E. Luppi, R. Magri, D. Ninno, O. Bisi, S. Ossicini, *Phys. Rev. B*, **69**, 155411 (2004).
- [8] Y. Ge, J.D. Head, *J. Phys. Chem. B*, **106**, 6997 (2002).
- [9] Y. Ge, J.D. Head, *Int. J. Quant. Chem.*, **95**, 617 (2003).
- [10] Y. Ge, J.D. Head, *J. Phys. Chem. B*, **108**, 6025 (2004).
- [11] Y. Ge, J.D. Head, *Chem. Phys. Lett.*, **398**, 107 (2004).
- [12] M.J.S. Dewar, E.G. Zoebisch, E.F. Healy, J.J.P. Stewart, *J. Am. Chem. Soc.*, **107**, 3902 (1985).
- [13] D.M. Deaven, K.M. Ho, *Phys. Rev. Lett.*, **75**, 288 (1995).
- [14] I. Rata, A.A. Shvartsburg, M. Horoi, T. Frauenheim, K.W.M. Siu, K.A. Jackson, *Phys. Rev. Lett.*, **85**, 546 (2000).
- [15] M.W. Schmidt, K.K. Baldridge, J.A. Boatz, S.T. Elbert, M.S. Gordon, J.H. Jensen, S. Koseki, N. Matsunaga, K.A. Nguyen, S. Su, T.L. Windus, M. Dupuis, J.A. Montgomery Jr., GAMESS, The General Atomic and Molecular Electronic Structure System, *J. Comput. Chem.*, **14**, 1347 (1993).
- [16] Y. Ge, J.D. Head, In preparation.
- [17] A.D. Becke, *J. Chem. Phys.*, **98**, 5648 (1993).
- [18] M.J. Frisch, G.W. Trucks, H.B. Schlegel, P.M.W. Gill, B.G. Johnson, M.A. Robb, J.R. Cheeseman, T. Keith, G.A. Petersson, J.A. Montgomery, K. Raghavachari, M.A. Al-Laham, V.G. Zakrzewski, J.V. Ortiz, J.B. Foresman, J. Cioslowski, B.B. Stefanov, A. Nanayakkara, M. Challacombe, C.Y. Peng, P.Y. Ayala, W. Chen, M.W. Wong, J.L. Andres, E.S. Replogle, R. Gomperts, R.L. Martin, D.J. Fox, J.S. Binkley, D.J. Defrees, J. Baker, J.P. Stewart, M. Head-Gordon, C. Gonzalez, J.A. Pople, Gaussian 94, Revision E.2, Gaussian, Inc., Pittsburgh, PA (1995).
- [19] W.R. Wadt, P.J. Hay, *J. chem. Phys.*, **82**, 284 (1985).
- [20] C.M. Rohlfing, K. Raghavachari, *Chem. Phys. Lett.*, **167**, 559 (1990).
- [21] T.H. Dunning Jr., P.J. Hay, In *Modern Theoretical Chemistry*, H.F. Schaefer (Ed.), Vol. 3, p. 1, Plenum, New York (1977).
- [22] C. Møller, M.S. Plesset, *Phys. Rev.*, **46**, 618 (1934).
- [23] L. Sari, M.C. McCarthy, H.F. Schaefer, P. Thaddeus, *J. Am. Chem. Soc.*, **125**, 11409 (2003).
- [24] G. Li, Q. Li, W. Xu, Y. Xie, H.F. Schaefer, *Molec. Phys.*, **99**, 1053 (2001).